Sensitive Fluorometric Detection of Fentanyl-Class Agents by Competition-Mediated Supramolecular Displacement and Graphene Nanoparticle Quenching

Yanjing Gao,[1] Farbod Shirinchi,[1] Audrey Hansrisuk,[1] Runyao Zhu,[1] Marya Lieberman,[2] Matthew J. Webber[1, *] and Yichun Wang[1, *]

[1]Department of Chemical and Biomolecular Engineering, University of Notre Dame, Notre Dame, Indiana 46556, United States

[2]Department of Chemistry and Biochemistry, University of Notre Dame, Notre Dame, Indiana 46556, United States

ABSTRACT: The emergence of synthetic opioids, and especially fentanyl and its analogues, has resulted in an epidemic of opioid abuse leading to a significant increase in overdose deaths in the United States, thus posing a threat to public health and safety. Current methods employed for the detection of fentanyl and its analogues have significant drawbacks in their sensitivity, scalability, and portability that limit use on a broader scale or in field-based application. The need to detect trace amounts of fentanyl in complex mixtures, and the continued emergence of new fentanyl analogues, further complicates these detection efforts. Accordingly, there is an urgent need to develop convenient, rapid, and reliable sensors for fentanyl detection. In this study, we have developed a fluorescent sensor based on the competitive displacement of a fluorophore (Hoechst 33342) from the cavity of a supramolecular macrocycle (cucurbit[7]uril), with subsequent fluorescence quenching from graphene quantum dots. This sensor can detect and quantify small quantities of fentanyl along with 58 fentanyl analogues, including detection of highly potent agents like carfentanil that are of increasing concern. Furthermore, the sensor achieves selective detection of these agents even when at 0.01 mol% in the presence of common interferents. In addition, the sensor provides results within seconds and offers stable performance over time. This simple, rapid, reliable, sensitive, and cost-effective sensor thus offers a valuable tool for detecting drugs in the fentanyl class, especially in the context of improving the effectiveness of field-based detection for law enforcement and military personnel in promoting public safety.

Introduction

The opioid epidemic, and in particular the abuse of fentanyl and its analogues, is a major public health crisis and also poses a serious threat to security.[1-2] Fentanyl is a potent synthetic opioid with anesthetic and analgesic function derived from binding and subsequent activation of the μ-opioid receptor,[3-4] with potency far-surpassing that of heroin (30-50 fold) and morphine (50-100 fold).[5-6] In addition, its high lipophilicity leads to enhanced brain distribution relative to these other agents.[7] The enhanced potency and more rapid action of fentanyl are beneficial for the treatment of severe pain, such as that associated with cancer or surgery.[8] However, these characteristics also lead to a high rate of physical dependence and addiction, with attendant risks for abuse and lethal overdose.[5] The accessible synthesis of fentanyl and its analogues has also made these agents pervasive as drugs of abuse, even including the inclusion of fentanyl in street drugs such as heroin or cocaine to boost their potency.[8-9] Drug users may unknowingly consume substantial quantities of fentanyl; with an estimated LD_{50} of only ~30 μg/kg,[10-11] its potency contributes to an alarming surge in fentanyl-related overdose deaths in the United States since 2013.[12] In 2022, fentanyl surpassed heroin to become the third most-seized drug and is currently a major contributor to drug-related overdose deaths in the United States.[13]

Combating this fentanyl crisis necessitates development of convenient, efficient, stable, and affordable tools to detect trace concentrations of fentanyl, including in complex mixtures with other drugs or inactive excipients.[6, 14-17] Currently available methods rely on liquid/gas chromatography-mass spectrometry (LC/GC-MS),[14, 18-19] quantitative nuclear magnetic resonance spectroscopy (qNMR),[20] and surface-enhanced Raman spectroscopy (SERS)[6, 21] for identification and quantification with high sensitivity and specificity, especially in analyzing fentanyl from complex mixtures. However, these techniques require expensive instrumentation operated by technically-trained experts in a laboratory setting; tedious pretreatment procedures and complicated surface modification techniques also present barriers to widespread implementation.[20] Alternatively, colorimetric tests,[22] immunoassays,[23-24] portable Raman spectrometers,[25] and handheld SERS devices[26] offer relative ease in operation, rapid response, and cost-effectiveness, However, many of these can be poorly quantitative, have low sensitivity, and struggle with detection of fentanyl in mixture due to both false-positive and false-negative results.[26-30] Lateral flow immunoassays offer a point-of-use approach to detect the presence of fentanyl, and though these rely on specific antibodies, their lack of molecular specificity yields false-positive results in the presence of high concentrations of

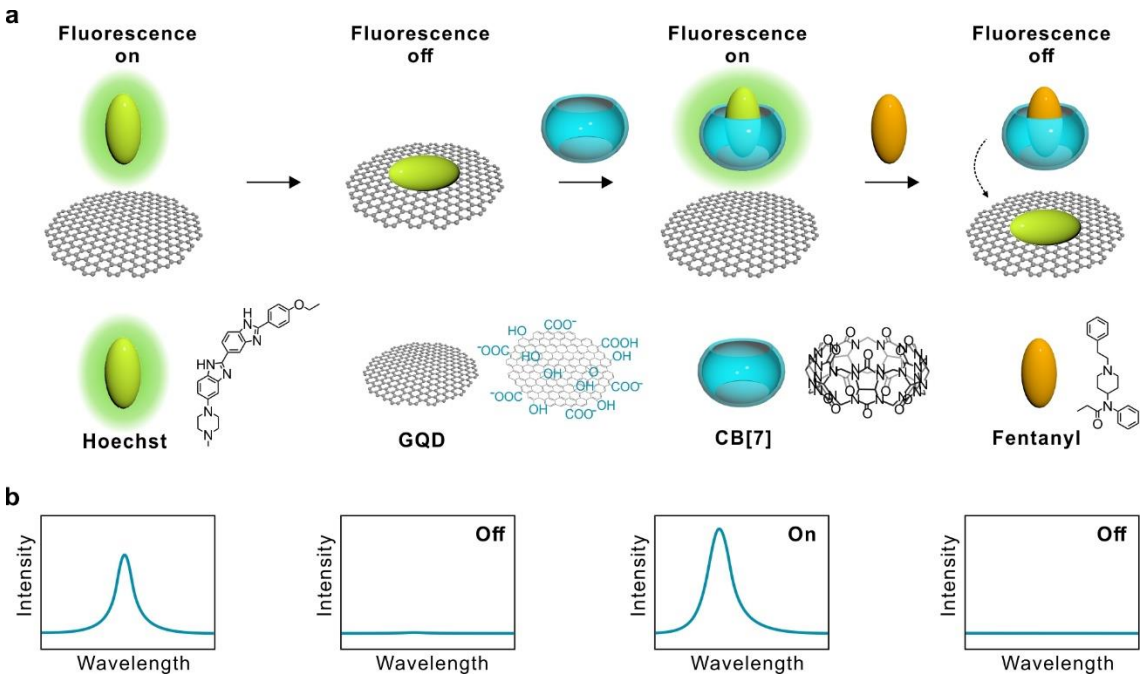

Scheme 1. Fentanyl detection based on an HO/GQD/CB[7] fluorescence sensor. (a) Scheme of the step-by-step assembly of the HO/GQD/CB[7] fluorescence sensor for fentanyl detection. (b) Illustrative demonstration of the expected HO fluorescence intensity following each step of the step-by-step sensor assembly and use for fentanyl detection.

interferents;[23-24] these can also struggle to detect certain fentanyl analogues with modifications to the 4-piperidinyl position (*e.g.,* carfentanil and 4-Phenyl fentanyl) or carbonyl moiety (*e.g.,* Despropionyl meta-Methylfentanyl and Despropionyl ortho-Fluorofentanyl).[23, 31-32] Accordingly, there remain ongoing challenges in achieving convenient, efficient, low-cost, stable, highly sensitive, and specific detection of fentanyl and its analogues in complex mixtures.

Supramolecular macrocycles offer opportunities for affinity-mediated capture and detection of certain small molecule analytes,[33] including fentanyl and related drugs of abuse.[34] One macrocycle in particular, cucurbit[7]uril (CB[7]), is a water-soluble host cavitand composed of seven repeating glycoluril units that offers high-affinity binding to a diverse array of small molecule guests.[35-37] The binding affinity of CB[7] has been investigated in diverse applications spanning drug delivery, sensing, imaging, nerve block reversal, protein isolation, and label-free enzyme assays.[38-42] CB[7] binds to the phenethylamine motif that is a characteristic feature of fentanyl and many of its analogues,[43] pointing to opportunities to use CB[7] for application in fentanyl sensing. For instance, covalently tethering CB[7] to the surface of silver nanoparticles for use in SERS detection enabled clear detection down to at least 0.5 nM. However, non-specific adsorption of the highly surface-active fentanyl to the colloid surface limits the utility of CB[7]-based selective capture for SERS detection. Another approach prepared a fluorescence sensor based on reversible aggregation of gold nanoclusters (AuNCs) using CB[7], with fentanyl binding reducing the extent of AuNC aggregation.[43] This sensor achieved a detection limit of ~3 nM with favorable selectivity in the presence of other illicit drugs, though relied on a complex design requiring peptide-modified AuNCs to achieve this function.

In this work, a CB[7]-based fluorescent sensor is demonstrated that offers a simple design, rapid and field-ready readout, and quantitative performance without need for tedious and expensive surface-modification of nanomaterials. This fluorescent fentanyl sensor (**Scheme 1**) is prepared by multi-step assembly of a fluorescent reporter (Hoechst 33342, HO), a quencher (graphene quantum dots, GQDs) and a fluorescence enhancer (CB[7]). HO is a cationic and weakly fluorescent dye in aqueous solution, yet exhibits a 20-fold increase in fluorescence quantum yield upon inclusion in the portal of CB[7]; the CB[7]–HO host–guest supramolecular complex has an affinity (K_{eq}) of 8.3 × 10^5 M^{-1} at neutral pH.[44] The free cationic HO dye readily adsorbs to negatively charged GQD, leading to a "turn off" in its fluorescence via energy transfer and quenching with the polyaromatic GQD. The addition of CB[7] to the HO/GQD complex desorbs HO through CB[7]–HO host–guest complexation, resulting in fluorescence "turn on" with enhancement relative to the fluorescence of HO alone in solution. When a guest with higher affinity for CB[7] binding, such as fentanyl (K_{eq} = 1.8 x 10^7 M^{-1})[34] is introduced to the HO/GQD/CB[7] mixture, fentanyl displaces HO, which again adsorbs to the GQD with quenching, leading to a fluorescence "turn off" response. The change in fluorescence from "on" to "off" enables quantitative detection of fentanyl down to nanomolar concentrations, including when in the presence of other drugs and adulterants. In addition, this detection method is

responsive to recognition of emerging and more potent fentanyl analogues that are becoming readily available.

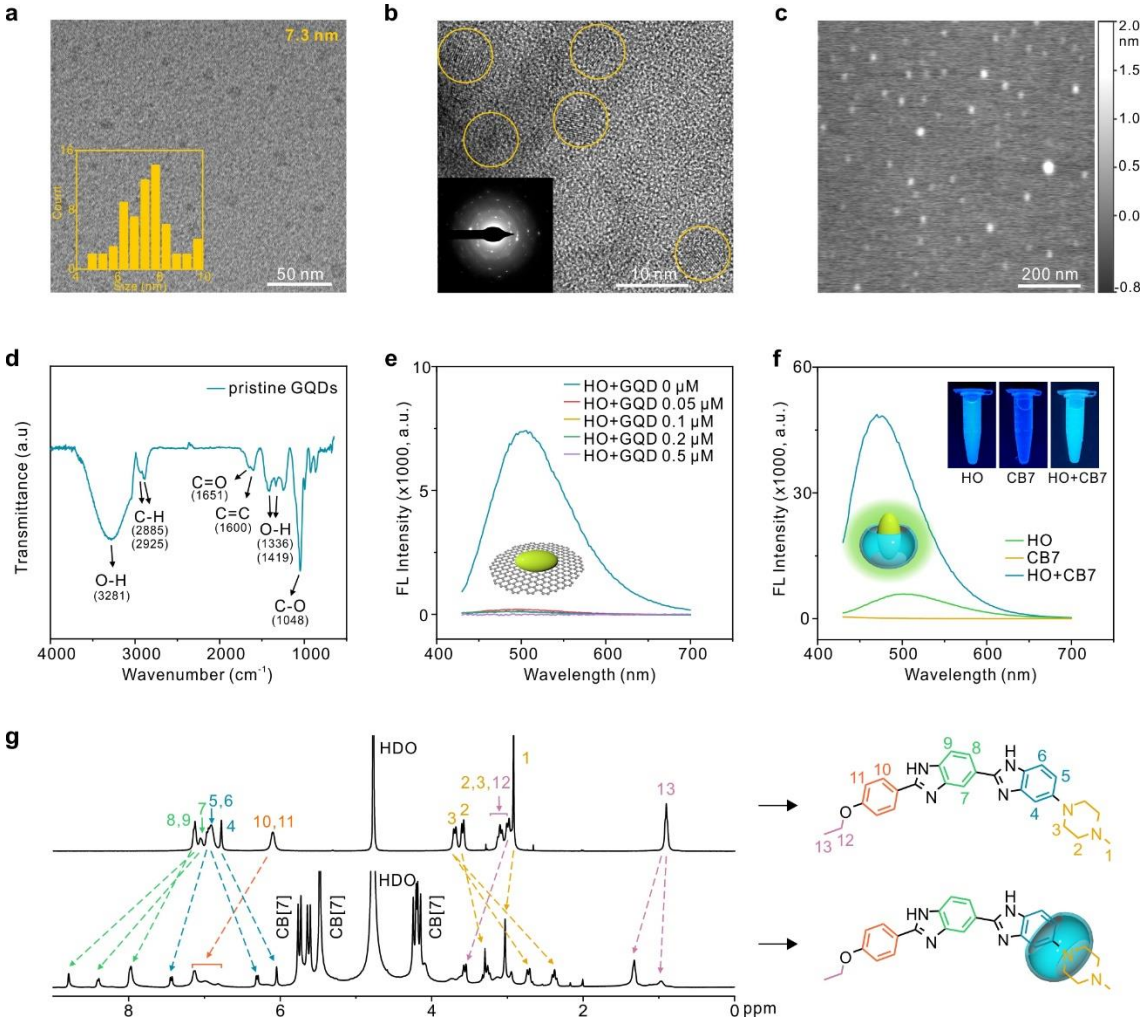

Figure 1. Characterization of sensor components of GQDs, HO, and CB[7]. (**a**) Transmission electron microscopy (TEM) image and size distribution (*inset*) of the pristine GQDs. (**b**) High-resolution TEM of the crystal lattice, with selected area electron diffraction (*inset*) of the pristine GQDs. (**c**) Atomic force microscopy (AFM) image, and (**d**) Fourier transform infrared (FTIR) spectrum of the pristine GQDs. (**e**) Fluorescence spectra of HO (0.25 μM) with GQD added at various concentrations (λ_{ex} = 350 nm). (**f**) Fluorescence spectra of HO, CB[7], and the CB[7]–HO complex (λ_{ex} = 350 nm). (**g**) ^{1}H NMR spectra of HO (*top*), and a 1:1 mixture of HO with CB[7] (*bottom*). Protons are labeled according to the structure shown, revealing the likely interaction mode of HO with CB[7].

Accordingly, selectivity in the presence of common interferents as well as the ability to recognize several other analogues in this drug class thereby improves on drawbacks of conventional immunoassays. In addition, this sensor provides rapid response times, with results available within seconds, and exhibits remarkable stability for over 20 days. This approach is furthermore amenable to detection of an assortment of fentanyl analogues. Given these attributes, this sensor has considerable promise as a high-throughput platform for routine and quantitative detection of fentanyl and its analogues.

Results and Discussion

Synthesis and characterization of sensor components. To construct a sensor, pristine GQDs were synthesized as the fluorescence quencher using modification of our previously reported methods.[45-46] The physical and chemical structure of the pristine GQDs were confirmed by a combination of microscopy and spectroscopy. High resolution transmission electron microscopy (TEM) revealed GQDs to have sizes of about 7.3 ± 1.2 nm (**Figure 1a**). In enlarged images (**Figure 1b**), the crystal lattice of graphene (~0.250 nm) was resolved, indicating a sample with highly crystalline nature. The thickness of GQDs was ~1 nm, as verified by atomic force microscopy (AFM, **Figure 1c**), corresponding to the expected thickness of a single layer. Fourier-transform infrared spectroscopy (FTIR) confirmed the presence of C=C, C=O, C–O, C–H, and O–H bonds on the GQDs (**Figure 1d**). The strongest absorption band at ~1048 cm^{-1} was associated with the stretching vibration of C–O bonds from surface hydroxyl groups.[47] The bands at ~1600 cm^{-1} and

~1651 cm^{-1} corresponded to the in-plane stretching vibrations of sp^2 hybridized carbon atoms (C=C), and the C=O stretching of carboxyl groups, respectively.[48] Furthermore, a broad absorption band at ~3281 cm^{-1} was attributed to stretching of the O–H of carboxyl groups.[48] Upon excitation (λ_{ex}) at 365 nm, GQDs showed an emission at 430-500 nm. The zeta potential of pristine GQDs was −21.0 ± 2.4 mV.

CB[7] was selected as a fluorescent enhancer, and synthesized according to established methodology.[49] To prepare the sensor, the CB[7] enhancer was paired with a fluorescent reporter dye that was also a guest for CB[7] binding. For the envisioned sensor design, the binding affinity of this reporter should be lower than the target analyte of interest, fentanyl in this case, to enable competition-mediated dye displacement for sensor read-out. Moreover, the dye must efficiently bind to the GQD quencher; the negative surface charge of the GQD offers a binding preference for positively charged dyes. According to these various design constraints, HO was selected as a cationic fluorescent guest of CB[7].[44] As depicted in **Figure 1e**, the fluorescence emission of HO was 480-520 nm (λ_{ex} = 350 nm). Addition of pristine GQDs resulted in a concentration-dependent "turn off" of HO fluorescence. These data point to an HO binding capacity of ~2.5 sites per 7.3 nm GQD particle. In spite of comparable excitation/emission profiles for HO and GQD, the fluorescence of the latter was negligible by comparison and could be readily subtracted as a background in all experiments. Combining HO with CB[7] in the absence of GQDs (**Figure 1f**) led to significant ~8 times enhancement in peak emission intensity, as well as a pronounced blue shift (from ~500 nm to ~470 nm). When in the presence of GQDs, the previously quenched fluorescence of HO could be effectively rescued upon addition of CB[7] (**Figure S1a**). The ^1H NMR spectra of HO demonstrated evidence of binding with CB[7], with shifting in specific protons pointing to a likely mode of inclusion complex formation involving portal alignment with the cationic tertiary amino groups on the HO (**Figure 1g**). A preference to bind HO by inclusion of nonpolar groups within the cavity and simultaneous electrostatic interactions between cationic charges on the guest and the electronegative carbonyls of the CB[7] portal aligns with expectations for CB[7]–guest binding. Importantly, the binding constant for the CB[7]–HO interaction (~10^5 M^{-1}) is lower than that reported for CB[7]–fentanyl (~10^7 M^{-1}).[34, 44] This facilitates a mechanism of fentanyl detection by competitive displacement of the HO dye from the CB[7] cavity, thus promoting the binding and concomitant quenching of HO by GQDs. In contrast, other cationic fluorescent dyes like Rhodamine B (RhB) and Acridine Orange (AO) did not offer optimal function. Under identical conditions, RhB was not effectively "turned off" by GQD, while AO was not desorbed and "turned on" by CB[7] addition (**Figure S1b,c**), in spite of the fact that AO is a guest for CB[7] with a moderate affinity of 2 × 10^5 M^{-1}.[50] As a result, HO was found to be an optimal fluorescence reporter for use in subsequent experiments.

Detection of model guests using HO/GQD/CB[7] sensor. To establish proof of principle for use of the HO/GQD/CB[7] sensor to detect fentanyl, a series of model guest analytes were first investigated, including hexamethylenediamine (HE), 3,3'-(octane-1,8-diyl)-bis-(1-ethyl-imidazolium) (BI), *p*-Xylylenediamine (PX), and 1-adamantanol (AD). These model guests have known binding affinities to CB[7] of ~10^7 M^{-1} (HE and BI), ~10^9 M^{-1} (PX), and ~10^{10} M^{-1} (AD).[51-52] The sensor was initially constructed through step-by-step assembly of HO, pristine GQDs, and CB[7], with a fixed molar concentration ratio of HO:GQD:CB[7] of 1:2:1. The successful construction was confirmed by distinct fluorescence transitions between "off" and "on" states upon addition of CB[7] (**Figure 2a, Figure S2**). Model guests were then introduced into the sensor system at a fixed molar concentration ratio of HO:GQD:CB[7]:model guest of 1:2:1:1. The introduction of model guests triggered competitive displacement of the HO dye from the CB[7] cavity, enabling rebinding of HO to pristine GQDs and yielding a nearly complete "turn off" of sensor fluorescence (**Figure 2a, Figure S2-S3**). Conversely, utilizing the CB[7]–HO complex as a sensor without quenching from pristine GQDs resulted in no quenching of HO fluorescence upon its competition-mediated displacement into solution, giving rise to a discernible background signal (**Figure S4**). Therefore, the established HO/GQD/CB[7] fluorescent sensor was an excellent candidate for model guest detection due to its enhanced signal-to-noise that resulted from coupling the fluorescent enhancement from the CB[7]–HO complex alongside quenching upon adsorption of displaced HO to GQDs.

We next defined the fluorescence switch-off efficiency, $(F_0\text{-}F)/F_0$, as a metric to quantify sensitivity, where F_0 and F represent the fluorescence of the sensor before and after the addition of model guests, respectively. Upon addition of known quantities of model guests, the sensor fluorescence decreased with increasing model guest concentration (**Figure 2b**). This calculation resulted in switch-off efficiency curves that displayed a linear relationship within the concentration range of 1-100 nM for the model guests (**Figure 2c,** *see SI methods for details on quantification*). The calculated limits of detection (LOD) derived from these linear relationships were 7.6 nM (HE), 9 nM (BI), 6.1 nM (PX), and 3.0 nM (AD). The low LODs suggested a highly sensitive detection capacity across a spectrum of model guests. Under identical conditions, the switch-off efficiency curves of model guests were established for CB[7]–HO in the absence of pristine GQDs, resulting in lower switch-off efficiency and higher limits of detection compared to that achieved by the HO/GQD/CB[7] sensor across various concentrations of model guest (**Figure S5**). This observation demonstrates the importance of including pristine GQDs as fluorescent quenchers to achieve heightened sensitivity from the HO/GQD/CB[7] sensor for model guest detection.

The sensor displayed an immediate response, as evidenced by recording fluorescence decay curves upon the addition of varying concentrations of model guest. The decay rate generally increased with higher concentrations of model guest and reached zero within a few minutes (**Figure 2d**). Remarkably, the decay rate was accelerated by mixing the mixtures after addition of model guest (**Figure S6a**). The fluorescence in the mixtures was already "off" upon detection, even though the manual operation time

from the adding the model guest to beginning data collection was strictly controlled to only 8 seconds, supporting a response time of a mere seconds. The duration of function for the sensor over time was studied by measuring the stability of its baseline "on" state over time.

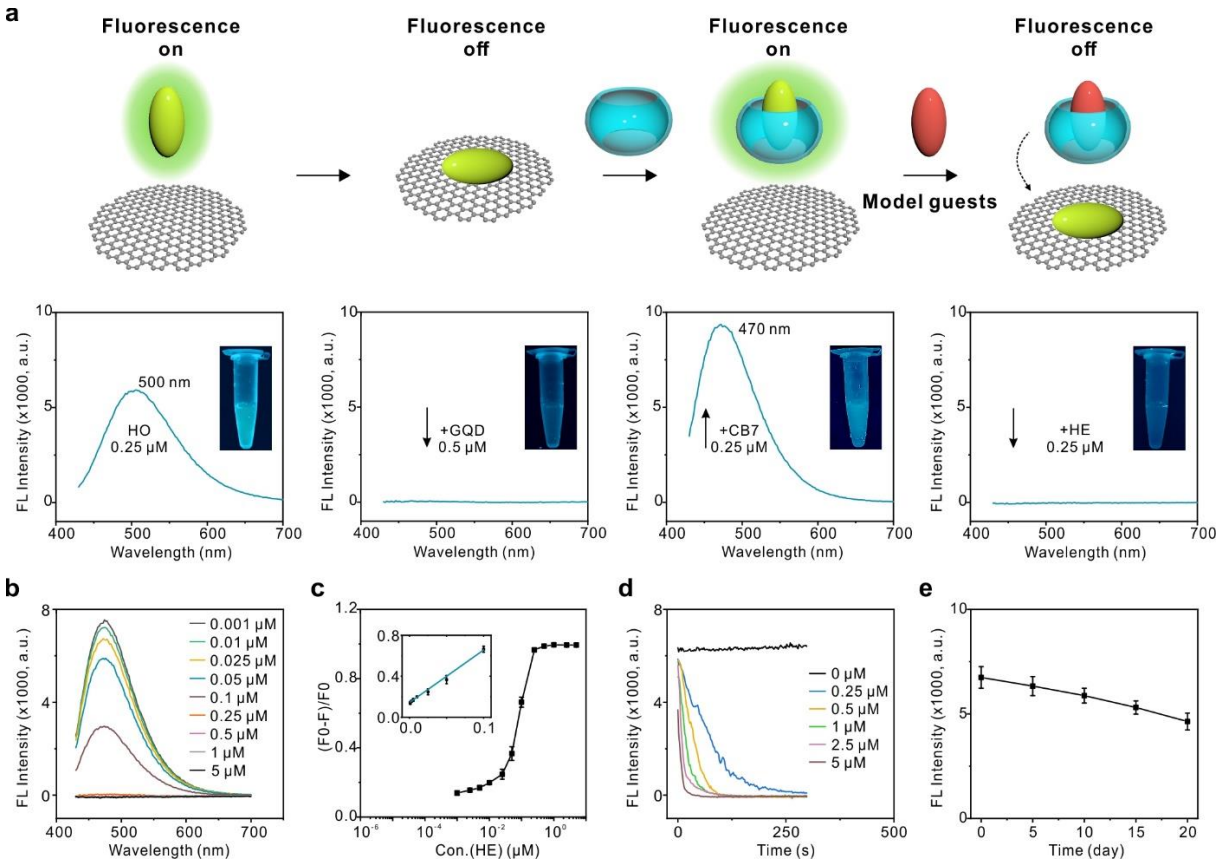

Figure 2. Performance of the HO/GQD/CB[7] sensor in detection of model guests. (a) Fluorescence toggling: "off" – "on" – "off" upon sequential addition of pristine GQDs, CB[7], and model guest (HE) into HO solution. (**b**) Fluorescence spectra of the sensor upon increasing the concentration of HE as a model guest. (**c**) Switch-off efficiency curve and linear response (*inset*) for assays using the sensor with varied concentrations of HE as a model guest. (**d**) Fluorescence response of the sensor upon the addition of HE as a model guest (λ_{ex}= 350 nm, λ_{em}= 470 nm). (**e**) Baseline fluorescence for the HO/GQD/CB[7] sensor over time.

Despite a decrease in fluorescence upon continuous monitoring for 20 d (**Figure 2e**), the sensor retained its high signal and rapid response capabilities (**Figure S6b**), supporting long-term stability. Comparatively, current methods based on LC/GC-MS,[14, 18-19] qNMR,[20] aptamer-based sensors,[53] CB[7]-based sensors,[43, 54] Ag-based SERS,[55] and immunoassays require time-intensive sample preparation, prolonged incubation times, and/or issues with long term stability.

Impact of GQD size and charge on sensor performance. To optimize sensor performance, GQDs with varying sizes were investigated as fluorescence quenchers. The size of GQDs were reported as an important factor governing their interaction with fluorescent dyes.[56-57] More importantly, this interaction plays a pivotal role in directly modulating both the "off" and "on" states of fluorescence in sensors, consequently influencing the fluorescence switch-off efficiency. Therefore, GQD size is potentially an influential factor that impacts the sensitivity of HO/GQD/CB[7] sensor. We synthesized GQDs with two additional sizes, 18.2 ± 2.7 nm and 36.2 ± 8.6 nm, respectively (**Figure 3a,b**). The corresponding zeta potential of the larger GQDs, named GQDs (18.2) and GQDs (36.2), were -15.1 ± 3.8 mV and -9.4 ± 2.8 mV, respectively (**Figure 3c**). The slight decrease in negative charges in larger GQDs compared to the smallest pristine GQDs is expected: while larger GQDs contain higher number of edge carboxylic groups proportional to their lateral size, the surface area of GQDs grows quadratically with their lateral size, thereby reducing the density of carboxylic groups.[57] Following characterization, GQDs with varying sizes were employed as fluorescence quenchers to explore sensing performance. In comparison with small pristine GQDs, it was observed that both larger GQDs (18.2 and 36.2) effectively "turn off" HO (**Figure 3d**). However, CB[7] could not efficiently "turn on" HO (**Figure 3e**), leading to a decreased fluorescence (F_0) of the sensors. Upon addition of

0.25 μM of the model guest (HE) into the sensor systems, HO was effectively quenched again (**Figure 3f**), resulting in a switch-off efficiency comparable to that in the small pristine GQD-based sensor (**Figure 3g**). Such phenomenon is supported by the calculated binding affinity of GQDs to HO (**Figure 3h,i**). Based on the analysis of fluorescence quenching data by nonlinear regression,[58] larger GQDs exhibited a stronger binding affinity to HO, with the order

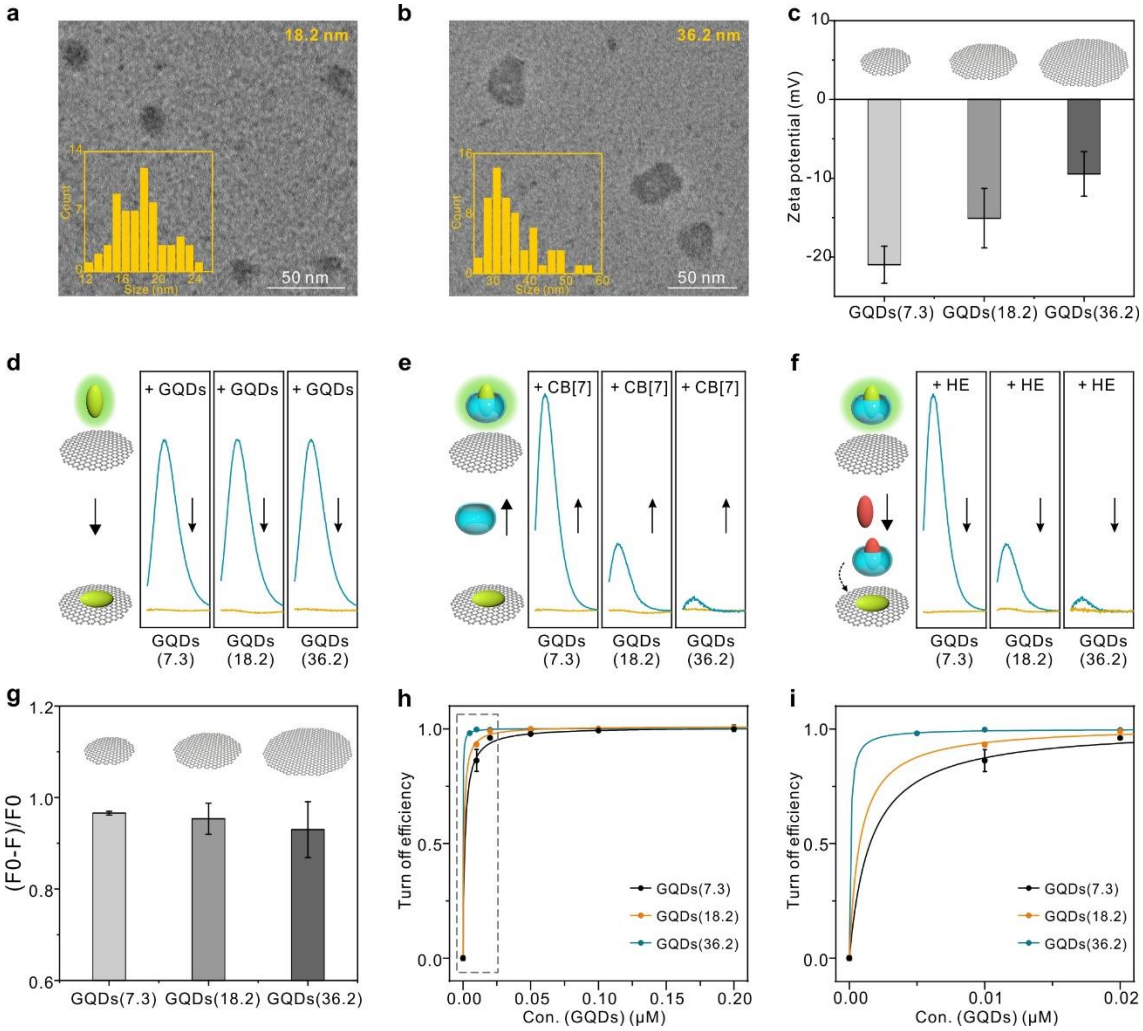

Figure 3. Impact of GQDs size on HO/GQD/CB[7] sensor performance. (**a-b**) TEM images and size distributions of GQDs in two distinct and larger size ranges of 18.2 nm (**a**) and 36.2 nm (**b**). (**c**) Zeta potentials of small pristine GQDs (7.3), medium GQDs (18.2), and large GQDs (36.2). (**d-f**) Fluorescence toggling: "off" – "on" – "off" upon addition of (**d**) 0.5 μM pristine GQD (7.3), GQD (18.2) or GQD (36.2) (*yellow*), (**e**) 0.25 μM CB[7] (*blue*), and (**f**) 0.25 μM HE (*yellow*) into HO solution. (**g**) Switch-off efficiency of the sensor prepared with pristine GQDs (7.3), GQDs (18.2), or GQDs (36.2). (**h**) The impact of GQDs concentration on the "Turn off efficiency" of HO. The "Turn off efficiency" was defined as $(F_{HO}-F_{HO+GQD})/F_{HO}$, where F_{HO} and F_{HO+GQD} represent the fluorescence of HO before and after the addition of GQDs. The binding affinities of HO to pristine GQDs (7.3), GQDs (18.2) and GQDs (36.2) were determined by GQDs concentration at 50% saturation of "Turn off efficiency", which were 1.51×10^{-6} M (7.3), 0.74×10^{-6} M (18.2), and 0.10×10^{-6} M (36.2). This indicates that the HO–GQDs binding affinity follows the order: pristine GQDs < GQDs (18.2) < GQDs (36.2). (**i**) The enlarged view of the grey-boxed area in (**h**).

GQDs (36.2) > GQDs (18.2) > pristine GQDs (**Figure 3h,i**). This enhanced binding affinity led to efficient "turn off" of HO, but made it challenging for CB[7] to compete with larger GQDs for HO binding. Consequently, despite larger GQD-based sensors achieving a high switch-off efficiency at the tested concentration of model guests, their low fluorescence intensity, dispersibility, and stability make them unsuitable for detection of competitive model guests.

Given the differing charges of small pristine GQDs, GQDs (18.2), and GQDs (36.2), further evaluations were necessary to understand the impact of charge variation on the performance of GQD-based sensors. The charge effect was thus assessed by altering the net charge of small pristine GQDs through addition of arginine surface ligands (**Figure S7a-c**).[45-46] In contrast to the pristine GQDs, Arg-GQDs with zeta potential of -2.0 ± 0.7 mV showed a reduction in switch-off efficiency (**Figure S7d-g**), potentially attributed to the

reduced negative charge of Arg-GQDs resulting in a lower binding affinity for the positively charged HO (**Figure S7h,i**). Taken together with data for GQD size, these results point to enhanced sensor performance characteristics for use of smaller and more negatively charged GQDs. Thus, smaller pristine GQD (7.3 ± 1.2 nm) with higher charge density, exceptional dispersibility, and stability provide the optimal quencher for use in HO/GQD/CB[7] sensors and these were chosen for use in fentanyl detection for all subsequent experiments.

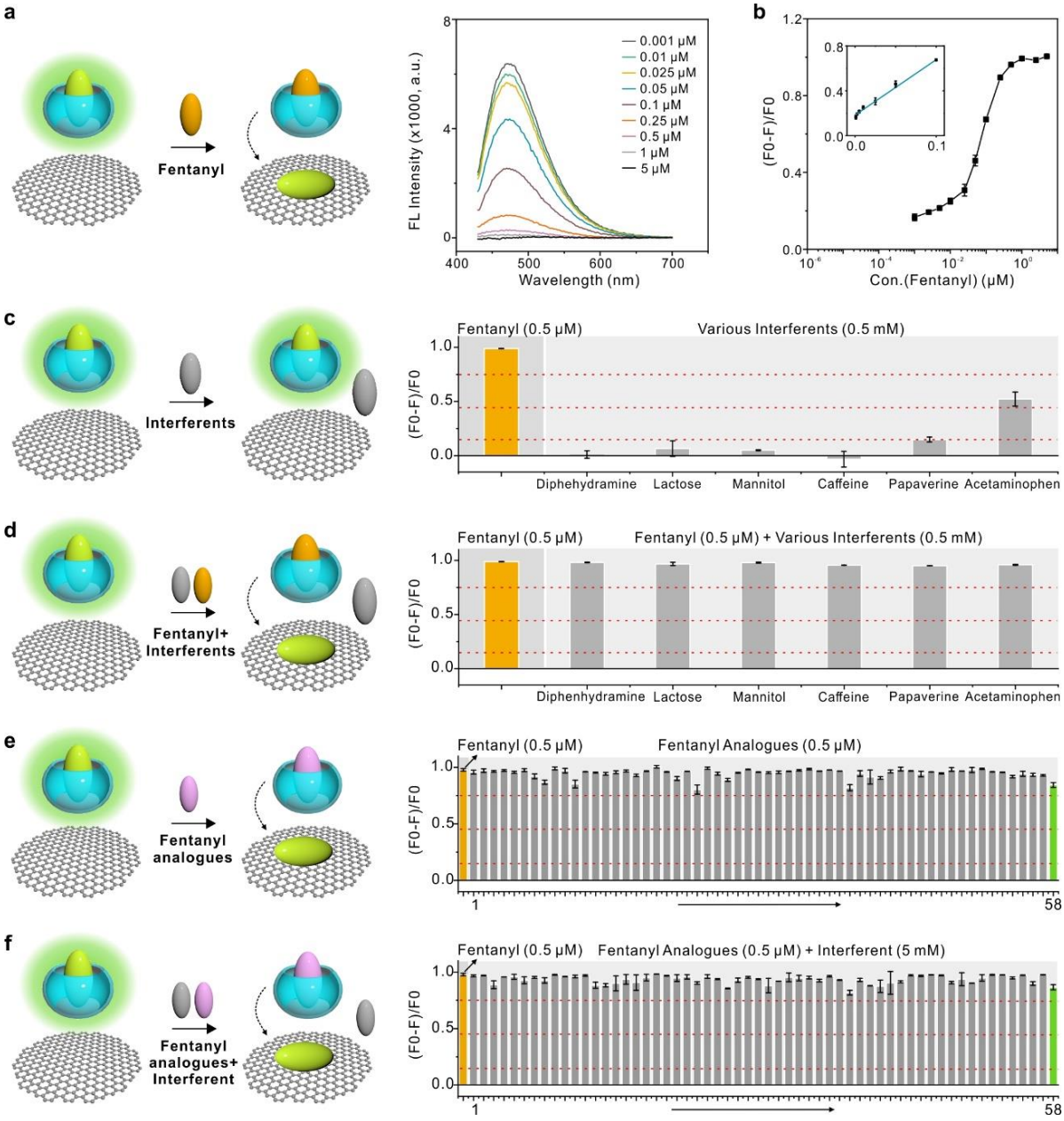

Figure 4. Sensitive and selective detection of fentanyl and fentanyl analogues using the HO/GQD/CB[7] sensor. (**a**) Fluorescence spectra of the sensor with fentanyl at increasing concentrations. (**b**) Switch-off efficiency curve and linear response (*inset*) for assays using the sensor with fentanyl at varied concentrations. (**c**) Specificity of the sensor in detecting fentanyl (0.5 μM) compared to its signal when exposed to various common interferents (0.5 mM). (**d**) Detection of fentanyl in binary mixtures containing 0.5 μM fentanyl with 0.5 mM other interferents. (**e**) Specificity of the sensor in detecting fentanyl (0.5 μM) as well as 58 fentanyl analogues (0.5 μM). Green bar represents carfentanil. The chemical structures of the tested 58 analogues were illustrated in **Figure S14**. (**f**) Detection of fentanyl analogues in binary mixtures containing 0.5 μM fentanyl analogues with 5 mM diphenhydramine as interferent. Green bar represents mixture of carfentanil and diphenhydramine. The red dashed lines in panels **c**-**f** indicate switch-off efficiency values of 0.15 (*bottom*), 0.45 (*middle*), 0.75 (*top*). The sensor response to testing samples was assessed based on switch-off efficiency, where the criteria were defined as follows: no response if switch-off efficiency < 0.15, low response if 0.15 < switch-off efficiency < 0.45, medium response if 0.45 < switch-off efficiency < 0.75, and high/significant response if switch-off efficiency > 0.75.

Detection of fentanyl and fentanyl analogues using HO/GQD/CB[7] sensor. The rapid, stable, and simple operation of the optimized HO/GQD/CB[7] presents a promising approach for fentanyl detection, effectively addressing the limitations in accessibility or reliability associated with conventional means of detection. To further evaluate this possibility, this sensor was first explored for fentanyl detection under the same conditions as those used for the model guests. Specifically, the concentration of the HO, pristine GQDs, and CB[7] were fixed at 0.25 μM, 0.5 μM, and 0.25 μM, respectively. The fentanyl concentration was then varied between 0.001–5 μM; the fluorescence emission peak at ~470 nm decreased upon increasing the concentration of fentanyl (**Figure 4a**). A complete fluorescence "off" state was observed for a fentanyl concentration of 0.5 μM and above. The switch-off efficiency from these emission spectra was then calculated, and from the resulting curve an LOD for fentanyl of 7.9 nM was derived (**Figure 4b**). By comparison, conventional immunoassay-based fentanyl test strips (FTS) using a lateral flow assay for qualitative detection of fentanyl have a practical detection limit greater than 50 nM (**Figure S8**).[24]

Sensor selectivity was next evaluated by testing the response to interferents at a greater molar concentration (5 mM) relative to fentanyl (0.5 μM), aiming to more accurately simulate the composition of real-world elicit drug formulations. Interferents tested included diphenhydramine, lactose, mannitol, caffeine, papaverine, and acetaminophen (*for chemical structures, see* **Figure S9**). Most of these interferent molecules produce no/low response even at concentrations up to millimolar (**Figure 4c, Figure S10**). The addition of diphenhydramine, lactose, mannitol, and caffeine to the sensor retained fluorescence identical to the blank without any interferents, yielding no response and thus had a fluorescence switch-off efficiency close to 0. Accordingly, the selected interferents were unable to competitively displace HO from the CB[7] cavity. Samples containing papaverine or acetaminophen yielded a small/medium value for switch-off efficiency at interferent concentrations up to 0.5 mM, suggesting that these compounds weakly interact with CB[7] to displace some HO at the concentrations tested. Nevertheless, fentanyl (0.5 μM) induced the most pronounced response, effectively turning off sensor fluorescence and also yielding the highest switch-off efficiency close to 1. In a comparison to the current standard for point-of-use detection technology, commercial FTS assays yielded false-positive results when diphenhydramine was at concentrations exceeding 0.5 mM (**Figure S11**). Hence, the HO/GQD/CB[7] sensor demonstrates enhanced reliability by mitigating false-positive responses from common co-formulation agents.

Given that fentanyl is often present at 1% by weight in drug samples prepared with many of the above-tested interferants,[53] the fluorescent sensor was next tested using binary mixtures of fentanyl and another interferent. In the binary mixtures, the fentanyl concentration was fixed at 0.5 μM, while the interferent concentration was varied from 0.5 μM to 5 mM. The sensor successfully detected fentanyl in all mixtures, producing a significant fluorescence response with a high switch-off efficiency close to 1 (**Figure 4d, Figure S12**). Fentanyl was also detectable in binary mixtures with varying concentrations of fentanyl (0.0025 - 0.5 μM) and fixed concentration of interferent (5 mM) (**Figure S13**). Remarkably, a low fluorescence response was observed even at a fentanyl concentration of 0.01 μM. These findings highlighted an exceptional ability to detect low levels of fentanyl in mixtures with interferents containing as low as 0.01 mol% fentanyl (0.5 μM in 5 mM interferent), therefore demonstrating high sensor selectivity under relevant formulation conditions.

Toward the introduction of more potent and addictive variants, the chemistry of fentanyl has also been varied in recent years.[59] For instance, carfentanil is ~100 times more potent than fentanyl and is now increasingly found in seized drugs and implicated in overdose deaths. Accordingly, the HO/GQD/CB[7] sensor was explored against 58 novel synthetic fentanyl analogues and intermediates with assorted structural modifications. These variants included carfentanil, acetyl fentanyl, *meta*-methyl cyclopropyl fentanyl, *para*-methoxy acetyl fentanyl, 4'-fluorofentanyl, *para*-methyl butyryl fentanyl, hexanoyl fentanyl, 3'-methyl acetyl fentanyl, N-benzyl phenyl norfentanyl, despropionyl *para*-fluorofentanyl, *meta*-fluoro valeryl fentanyl, furanyl fentanyl, and others (*for chemical structures, see* **Figure S14**). When tested at 0.5 μM, all of these fentanyl analogues produced a significant "turn-off" response in sensor fluorescence, yielding a high switch-off efficiency (**Figure 4e**). Excitingly, the HO/GQD/CB[7] sensor was able to detect fentanyl analogues that cannot be detected by commercially used FTS, such as carfentanil, 4-Phenyl fentanyl, Despropionyl meta-Methylfentanyl, Despropionyl ortho-Fluorofentanyl, Despropionyl para-Fluorofentanyl, 4-Anilino-1-Boc-piperidine, Despropionyl 2'-fluoro ortho-Fluorofentanyl, para-fluoro 4-ANBP.[23, 31-32] The HO/GQD/CB[7] sensor was also tested with binary mixtures of all 58 fentanyl analogues (0.5 μM) and an interferent of diphenhydramine at 5 mM (**Figure 4f**). Again, the sensor could detect all 58 analogues at 0.01 mol% in these drug mixtures. These observations demonstrated excellent detection performance with the capacity to detect at least 58 fentanyl analogues, even in drug mixtures predominated by interferents. Accordingly, this HO/GQD/CB[7]-based fluorescence sensor offers a highly sensitive and selective detection tool for trace amounts of fentanyl and its analogues in relevant drug mixtures.

Conclusions

Fentanyl and related opioid analogues are responsible for the majority of drug overdose deaths in the United States. Their high potency and accessibility furthermore pose a concern for use as chemical agents. Given widespread use and exposure risk, the development of simple, rapid, reliable, and cost-effective detection tools is essential for forensics, medical care, and public safety. In this work, a fluorescence sensor was developed to detect fentanyl and its analogues by using step-by-step assembly of HO, GQD, and CB[7]. The sensor provided a fluorescence "turn-off" response enabling detection and quantification of fentanyl down to 7.9 nM. The sensor also offered robust performance in detecting fentanyl in mixtures with other interferents, even in cases where fentanyl was at a

concentration of only 0.01 mol% relative to the interferent. Its sensitivity and specificity arises from rapid and selective host–guest complex formation between CB[7] and fentanyl, along with a low background from the fluorescence quenching of a displaced fluorescence reporter using GQDs. Indeed, this affinity-based recognition method outperforms standard FTS immunoassays, which only qualitatively detect fentanyl at concentrations of 50 nM or higher and yield false-positive results in the presence of these same interferents. The extensibility of this sensor to detect emergent threats was further evident in its ability to recognize 58 fentanyl analogues, even in mixtures with interferents. This sampling included detection of carfentanil, which presents an emerging threat given its increased availability and potency that is ~100x that of fentanyl. The sensor demonstrated rapid response time with results achieved in seconds, as well as exceptional stability over a period of 20+ days. The mode of detection should furthermore be amenable to integration with low-cost and field-ready detection methodologies. Accordingly, this sensor offers promise as a rapid, point-of-use platform for routine and quantitative detection of fentanyl and its analogues.

ASSOCIATED CONTENT

Supporting Information

This material is available free of charge via the Internet at http://pubs.acs.org.

Experimental materials and methods. Supplementary data for the construction of HO/GQD/CB[7] sensor, detection of model guests by HO/GQD/CB[7] sensor and HO/CB[7] complex, fluorescence response of HO/GQD/CB[7] sensor, impact of GQDs charge on HO/GQD/CB[7] sensor performance, chemical structures of interferents and fentanyl analogues, FTS response to fentanyl and diphenhydramine, selectivity testing for interferents and binary mixtures containing fentanyl with interferents.

AUTHOR INFORMATION

Corresponding Authors

Yichun Wang - Department of Chemical and Biomolecular Engineering, University of Notre Dame, Notre Dame, Indiana 46556, United States; orcid.org/0000-0002-4353-6660; E-mail: ywang65@nd.edu.

Matthew J. Webber - Department of Chemical and Biomolecular Engineering, University of Notre Dame, Notre Dame, Indiana 46556, United States; orcid.org/0000-0003-3111-6228; E-mail: mwebber@nd.edu.

Authors

Yanjing Gao – Department of Chemical and Biomolecular Engineering, University of Notre Dame, Notre Dame, Indiana 46556, United States; orcid.org/0000-0003-2317-0726.

Farbod Shirinchi - Department of Chemical and Biomolecular Engineering, University of Notre Dame, Notre Dame, Indiana 46556, United States.

Audrey Hansrisuk - Department of Chemical and Biomolecular Engineering, University of Notre Dame, Notre Dame, Indiana 46556, United States.

Runyao Zhu - Department of Chemical and Biomolecular Engineering, University of Notre Dame, Notre Dame, Indiana 46556, United States.

Marya Lieberman - Department of Chemistry and Biochemistry, University of Notre Dame, Notre Dame, Indiana 46556, United States; orcid.org/0000-0003-3968-8044.

Author Contributions

Y.W. and M.W. conceptualized the project. Y.W. and Y.G. designed the experiments, analyzed data, wrote and revised the manuscript. Y.G. performed the experiments. F.S. synthesized larger GQDs and drew the structures of GQDs and fentanyl analogues. A.H. performed the NMR measurements. R.Z. performed TEM, AFM and FTIR measurements. M.L. provided fentanyl and fentanyl analogues and advice on study design. All authors have given approval to the final version of the manuscript.

Notes

The authors declare no competing financial interest.

ACKNOWLEDGMENT

The authors gratefully acknowledge the financial support from a Seed Fund of The Berthiaume Institute for Precision Health at the University of Notre Dame.

REFERENCES

(1) Williams, D. R.; Etkins, O. S., Racism and mental health. *World Psychiatry* **2021,** *20* (2), 194-195.

(2) Kelly, E.; Sutcliffe, K.; Cavallo, D.; Ramos-Gonzalez, N.; Alhosan, N.; Henderson, G., The anomalous pharmacology of fentanyl. *Br. J. Pharmacol.* **2021,** *180* (7), 797-812.

(3) Zhuang, Y.; Wang, Y.; He, B.; He, X.; Zhou, X. E.; Guo, S.; Rao, Q.; Yang, J.; Liu, J.; Zhou, Q.; Wang, X.; Liu, M.; Liu, W.; Jiang, X.; Yang, D.; Jiang, H.; Shen, J.; Melcher, K.; Chen, H.; Jiang, Y.; Cheng, X.; Wang, M.-W.; Xie, X.; Xu, H. E., Molecular recognition of morphine and fentanyl by the human μ-opioid receptor. *Cell* **2022,** *185* (23), 4361-4375.

(4) Vo, Q. N.; Mahinthichaichan, P.; Shen, J.; Ellis, C. R., How μ-opioid receptor recognizes fentanyl. *Nat. Commun.* **2021,** *12*, 984.

(5) Han, Y.; Yan, W.; Zheng, Y.; Khan, M. Z.; Yuan, K.; Lu, L., The rising crisis of illicit fentanyl use, overdose, and potential therapeutic strategies. *Transl. Psychiatry* **2019,** *9* (1), 282-290.

(6) Su, X.; Liu, X.; Xie, Y.; Chen, M.; Zhong, H.; Li, M., Quantitative Label-Free SERS Detection of Trace Fentanyl in Biofluids with a Freestanding Hydrophobic Plasmonic Paper Biosensor. *Anal. Chem.* **2023,** *95* (7), 3821-3829.

(7) Comer, S. D.; Cahill, C. M., Fentanyl: Receptor pharmacology, abuse potential, and implications for treatment. *Neurosci. Biobehav. Rev.* **2019,** *106*, 49-57.

(8) Stanley, T. H., The Fentanyl Story. *J. Pain* **2014,** *15* (12), 1215-1226.

(9) Pergolizzi, J.; Magnusson, P.; LeQuang, J. A. K.; Breve, F., Illicitly Manufactured Fentanyl Entering the United States. *Cureus* **2021,** *13* (8), e17496.

(10) Smith, L. C.; Bremer, P. T.; Hwang, C. S.; Zhou, B.; Ellis, B.; Hixon, M. S.; Janda, K. D., Monoclonal Antibodies for Combating Synthetic Opioid Intoxication. *J. Am. Chem. Soc.* **2019,** *141* (26), 10489-10503.

(11) Barrientos, R. C.; Bow, E. W.; Whalen, C.; Torres, O. B.; Sulima, A.; Beck, Z.; Jacobson, A. E.; Rice, K. C.; Matyas, G. R., Novel Vaccine That Blunts Fentanyl Effects and Sequesters Ultrapotent Fentanyl Analogues. *Mol. Pharm.* **2020,** *17* (9), 3447-3460.

(12) O'Donnell, J. K.; Halpin, J.; Mattson, C. L.; Goldberger, B. A.; Gladden, R. M. *Deaths Involving Fentanyl, Fentanyl Analogs, and U-47700-10 States, July-December 2016*; US Department of Health and Human Services/Centers for Disease Control and Prevention: November 2017.

(13) Division., D. C. *National Forensic Laboratory Information System: NFLIS-Drug 2022 annual report.*; U.S. Department of Justice, U.S. Drug Enforcement Administration.: 2023.

(14) Palmquist, K. B.; Truver, M. T.; Shoff, E. N.; Krotulski, A. J.; Swortwood, M. J., Review of analytical methods for screening and quantification of fentanyl analogs and novel synthetic opioids in biological specimens. *J. Forensic Sci.* **2023,** *68* (5), 1643-1661.

(15) Crocombe, R. A.; Giuntini, G.; Schiering, D. W.; Profeta, L. T. M.;

Hargreaves, M. D.; Leary, P. E.; Brown, C. D.; Chmura, J. W., Field-portable detection of fentanyl and its analogs: A review. *J. Forensic Sci.* **2023,** *68* (5), 1570-1600.
(16) Angelini, D. J.; Biggs, T. D.; Prugh, A. M.; Smith, J. A.; Hanburger, J. A.; Llano, B.; Avelar, R.; Ellis, A.; Lusk, B.; Malik Naanaa, A.; Sisco, E.; Sekowski, J. W., The use of lateral flow immunoassays for the detection of fentanyl in seized drug samples and postmortem urine. *J. Forensic Sci.* **2020,** *66* (2), 758-765.
(17) Zhang, M.; Pan, J.; Xu, X.; Fu, G.; Zhang, L.; Sun, P.; Yan, X.; Liu, F.; Wang, C.; Liu, X.; Lu, G., Gold-Trisoctahedra-Coated Capillary-Based SERS Platform for Microsampling and Sensitive Detection of Trace Fentanyl. *Anal. Chem.* **2022,** *94* (11), 4850-4858.
(18) Buchalter, S.; Marginean, I.; Yohannan, J.; Lurie, I. S., Gas chromatography with tandem cold electron ionization mass spectrometric detection and vacuum ultraviolet detection for the comprehensive analysis of fentanyl analogues. *J. Chromatogr.* **2019,** *1596*, 183-193.
(19) Zhang, Y.; Halifax, J. C.; Tangsombatvisit, C.; Yun, C.; Pang, S.; Hooshfar, S.; Wu, A. H. B.; Lynch, K. L., Development and application of a High-Resolution mass spectrometry method for the detection of fentanyl analogs in urine and serum. *JMSACL* **2022,** *26*, 1-6.
(20) McCrae, K.; Tobias, S.; Grant, C.; Lysyshyn, M.; Laing, R.; Wood, E.; Ti, L., Assessing the limit of detection of Fourier-transform infrared spectroscopy and immunoassay strips for fentanyl in a real-world setting. *Drug Alcohol Rev.* **2019,** *39* (1), 98-102.
(21) Qin, Y.; Yin, S.; Chen, M.; Yao, W.; He, Y., Surface-enhanced Raman spectroscopy for detection of fentanyl and its analogs by using Ag-Au nanoparticles. *Spectrochim. Acta A Mol. Biomol. Spectrosc.* **2023,** *285*, 121923.
(22) Lin, Y.; Sun, J.; Tang, M.; Zhang, G.; Yu, L.; Zhao, X.; Ai, R.; Yu, H.; Shao, B.; He, Y., Synergistic Recognition-Triggered Charge Transfer Enables Rapid Visual Colorimetric Detection of Fentanyl. *Anal. Chem.* **2021,** *93* (16), 6544-6550.
(23) Park, J. N.; Sherman, S. G.; Sigmund, V.; Breaud, A.; Martin, K.; Clarke, W. A., Validation of a lateral flow chromatographic immunoassay for the detection of fentanyl in drug samples. *Drug Alcohol Depend.* **2022,** *240*, 109610.
(24) Lockwood, T.-L. E.; Vervoordt, A.; Lieberman, M., High concentrations of illicit stimulants and cutting agents cause false positives on fentanyl test strips. *Harm. Reduct. J.* **2021,** *18* (1), 30.
(25) Gozdzialski, L.; Ramsay, M.; Larnder, A.; Wallace, B.; Hore, D. K., Fentanyl detection and quantification using portable Raman spectroscopy in community drug checking. *J. Raman Spectrosc.* **2021,** *52* (7), 1308-1316.
(26) Smith, M.; Logan, M.; Bazley, M.; Blanchfield, J.; Stokes, R.; Blanco, A.; McGee, R., A Semi-quantitative method for the detection of fentanyl using surface-enhanced Raman scattering (SERS) with a handheld Raman instrument. *J. Forensic Sci.* **2020,** *66* (2), 505-519.
(27) O'Neal, C. L.; Crouch, D. J.; Fatah, A. A., Validation of twelve chemical spot tests for the detection of drugs of abuse. *Forensic Sci. Int.* **2000,** *109* (3), 189-201.
(28) Ott, C. E.; Burns, A.; Sisco, E.; Arroyo, L. E., Targeted fentanyl screening utilizing electrochemical surface-enhanced Raman spectroscopy (EC-SERS) applied to authentic seized drug casework samples. *Forensic Chem.* **2023,** *34*, 100492.
(29) Hargreaves, M., *Handheld Raman, SERS, and SORS*. John Wiley & Sons, Ltd.: 2021.
(30) Wilson, N. G.; Raveendran, J.; Docoslis, A., Portable identification of fentanyl analogues in drugs using surface-enhanced Raman scattering. *Sensors Actuators B: Chem.* **2021,** *330*, 129303.
(31) Hayes, K. L.; Lieberman, M., Assessment of two brands of fentanyl test strips with 251 synthetic opioids reveals "blind spots" in detection capabilities. *Harm. Reduct. J.* **2023,** *20* (1), 175.
(32) Rodriguez-Cruz, S. E., Evaluating the sensitivity, stability, and cross-reactivity of commercial fentanyl immunoassay test strips. *J. Forensic Sci.* **2023,** *68* (5), 1555-1569.
(33) Hennig, A.; Bakirci, H.; Nau, W. M., Label-free continuous enzyme assays with macrocycle-fluorescent dye complexes. *Nat. Methods* **2007,** *4* (8), 629-632.
(34) Ganapati, S.; Grabitz, S. D.; Murkli, S.; Scheffenbichler, F.; Rudolph, M. I.; Zavalij, P. Y.; Eikermann, M.; Isaacs, L., Molecular Containers Bind Drugs of Abuse in Vitro and Reverse the Hyperlocomotive Effect of Methamphetamine in Rats. *ChemBioChem* **2017,** *18* (16), 1583-1588.
(35) Barrow, S. J.; Kasera, S.; Rowland, M. J.; del Barrio, J.; Scherman, O. A., Cucurbituril-Based Molecular Recognition. *Chem. Rev.* **2015,** *115* (22), 12320-12406.
(36) Lee, J. W.; Samal, S.; Selvapalam, N.; Kim, H.-J.; Kim, K., Cucurbituril homologues and derivatives: new opportunities in supramolecular chemistry. *Acc. Chem. Res.* **2003,** *36* (8), 621-630.
(37) Assaf, K. I.; Nau, W. M., Cucurbiturils: from synthesis to high-affinity binding and catalysis. *Chem. Soc. Rev.* **2015,** *44* (2), 394-418.
(38) Deng, C.-L.; Murkli, S. L.; Isaacs, L. D., Supramolecular hosts as in vivo sequestration agents for pharmaceuticals and toxins. *Chem. Soc. Rev.* **2020,** *49* (21), 7516-7532.
(39) Lee, D.-W.; Park, K. M.; Banerjee, M.; Ha, S. H.; Lee, T.; Suh, K.; Paul, S.; Jung, H.; Kim, J.; Selvapalam, N.; Ryu, S. H.; Kim, K., Supramolecular fishing for plasma membrane proteins using an ultrastable synthetic host–guest binding pair. *Nat. Chem.* **2010,** *3* (2), 154-159.
(40) Liu, Y. C.; Peng, S.; Angelova, L.; Nau, W. M.; Hennig, A., Label-Free Fluorescent Kinase and Phosphatase Enzyme Assays with Supramolecular Host-Dye Pairs. *ChemistryOpen* **2019,** *8* (11), 1350-1354.
(41) Bockus, A. T.; Smith, L. C.; Grice, A. G.; Ali, O. A.; Young, C. C.; Mobley, W.; Leek, A.; Roberts, J. L.; Vinciguerra, B.; Isaacs, L.; Urbach, A. R., Cucurbit[7]uril–Tetramethylrhodamine Conjugate for Direct Sensing and Cellular Imaging. *J. Am. Chem. Soc.* **2016,** *138* (50), 16549-16552.
(42) Zou, L.; Braegelman, A. S.; Webber, M. J., Spatially Defined Drug Targeting by in Situ Host–Guest Chemistry in a Living Animal. *ACS Cent. Sci.* **2019,** *5* (6), 1035-1043.
(43) Yan, K.; Wang, L.; Zhu, Z.; Duan, S.; Hua, Z.; Xu, P.; Xu, H.; Hu, C.; Wang, Y.; Di, B., Cucurbituril-protected dual-readout gold nanoclusters for sensitive fentanyl detection. *Analyst* **2023,** *148* (6), 1253-1258.
(44) Wang, Q.; Lü, L.-B.; Tao, Z.; Sun, T.; Tang, Q.; Huang, Y., The pH and mercury ion stimuli-responsive supramolecular assemblies of cucurbit[7]uril and Hoechst 33342. *Spectrochim. Acta A Mol. Biomol. Spectrosc.* **2021,** *254*, 119656.
(45) Suzuki, N.; Wang, Y.; Elvati, P.; Qu, Z.-B.; Kim, K.; Jiang, S.; Baumeister, E.; Lee, J.; Yeom, B.; Bahng, J. H.; Lee, J.; Violi, A.; Kotov, N. A., Chiral Graphene Quantum Dots. *ACS Nano* **2016,** *10* (2), 1744-1755.
(46) Zhang, Y.; Kim, G.; Zhu, Y.; Wang, C.; Zhu, R.; Lu, X.; Chang, H.-C.; Wang, Y., Chiral Graphene Quantum Dots Enhanced Drug Loading into Small Extracellular Vesicles. *ACS Nano* **2023,** *17* (11), 10191-10205.
(47) Zhu, R.; Makwana, K. M.; Zhang, Y.; Rajewski, B. H.; Del Valle, J. R.; Wang, Y., Blocking tau transmission by biomimetic graphene nanoparticles. *J. Mater. Chem. B* **2023,** *11* (31), 7378-7388.
(48) Saleem, H.; Saud, A.; Zaidi, S. J., Sustainable Preparation of Graphene Quantum Dots from Leaves of Date Palm Tree. *ACS Omega* **2023,** *8* (31), 28098-28108.
(49) Kim, J.; Jung, I. S.; Kim, S. Y.; Lee, E.; Kang, J. K.; Sakamoto, S.; Yamaguchi, K.; Kim, K., New cucurbituril homologues:: Syntheses, isolation, characterization, and X-ray crystal structures of cucurbit[n]uril (n=5, 7, and 8). *J. Am. Chem. Soc.* **2000,** *122* (3), 540-541.
(50) Shaikh, M.; Mohanty, J.; Singh, P. K.; Nau, W. M.; Pal, H., Complexation of acridine orange by cucurbit[7]uril and β-cyclodextrin:: photophysical effects and pKa shifts. *Photochem. Photobiol. Sci.* **2008,** *7* (4), 408-414.
(51) Moghaddam, S.; Yang, C.; Rekharsky, M.; Ko, Y. H.; Kim, K.; Inoue, Y.; Gilson, M. K., New Ultrahigh Affinity Host-Guest Complexes of Cucurbit[7]uril with Bicyclo[2.2.2]octane and Adamantane Guests: Thermodynamic Analysis and Evaluation of M2 Affinity Calculations. *J. Am. Chem. Soc.* **2011,** *133* (10), 3570-3581.
(52) Liu, S. M.; Ruspic, C.; Mukhopadhyay, P.; Chakrabarti, S.; Zavalij, P. Y.; Isaacs, L., The cucurbit[n]uril family: Prime components for self-sorting systems. *J. Am. Chem. Soc.* **2005,** *127* (45), 15959-15967.
(53) Canoura, J.; Liu, Y.; Perry, J.; Willis, C.; Xiao, Y., Suite of Aptamer-Based Sensors for the Detection of Fentanyl and Its Analogues. *ACS Sens.* **2023,** *8* (5), 1901-1911.
(54) Selective Capture and Detection of Fentanyl with Modified Cucurbit[7]uril Macrocycles.
(55) Yang, Y.; Liu, J.; Fu, Z.-W.; Qin, D., Galvanic Replacement-Free Deposition of Au on Ag for Core–Shell Nanocubes with Enhanced Chemical Stability and SERS Activity. *J. Am. Chem. Soc.* **2014,** *136* (23), 8153-8156.
(56) Ibarbia, A.; Grande, H. J.; Ruiz, V., On the Factors behind the Photocatalytic Activity of Graphene Quantum Dots for Organic Dye Degradation. *Part. Part. Syst. Char.* **2020,** *37* (5), 2000061.

(57) Zhang, F.; Liu, F.; Wang, C.; Xin, X.; Liu, J.; Guo, S.; Zhang, J., Effect of Lateral Size of Graphene Quantum Dots on Their Properties and Application. *ACS Appl. Mater. Interfaces* **2016,** *8* (3), 2104-2110.
(58) Rawel, H. M.; Frey, S. K.; Meidtner, K.; Kroll, J.; Schweigert, F. J., Determining the binding affinities of phenolic compounds to proteins by quenching of the intrinsic tryptophan fluorescence. *Mol. Nutr. Food Res.* **2006,** *50* (8), 705-713.
(59) Armenian, P.; Vo, K. T.; Barr-Walker, J.; Lynch, K. L., Fentanyl, fentanyl analogs and novel synthetic opioids: A comprehensive review. *Neuropharmacology* **2018,** *134*, 121-132.